The aorta in transposition of the great arteries

Palen, R.L.F. van der

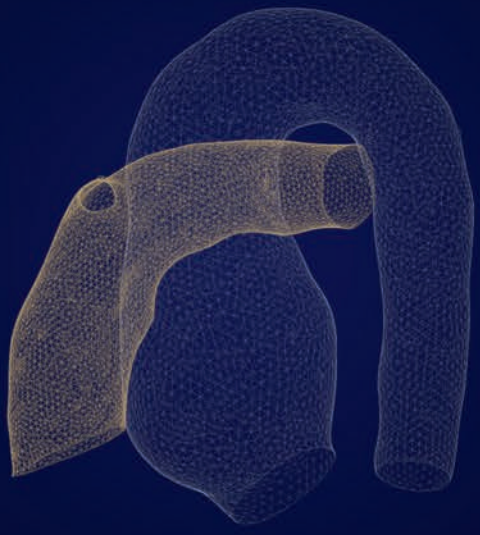

CHAPTER 8

Wall shear stress in the thoracic aorta at rest and with dobutamine stress after arterial switch operation

European Journal of Cardio-Thoracic Surgery. 2021;59:814-22

Roel L.F. van der Palen
Joe F. Juffermans
Lucia J.M. Kroft
Mark G. Hazekamp
Hildo J. Lamb
Nico A. Blom
Arno A.W. Roest
Jos J.M. Westenberg

Abstract

Objectives

Progressive root dilatation is an important complication in patients with transposition of the great arteries (TGA) after arterial switch operation (ASO) that may be caused by altered flow dynamics. Aortic wall shear stress (WSS) distribution at rest and under dobutamine stress (DS) conditions using 4D flow magnetic resonance imaging (MRI) were investigated in relation to thoracic aorta geometry.

Methods

4D flow MRI was performed in sixteen adolescent TGA patients after ASO (rest and DS condition) and in ten healthy controls (rest). The primary outcome measure was the WSS distribution along the aortic segments and the WSS change with DS in TGA patients. Based on the results, we secondary zoomed in on factors (aortic geometry and left ventricular (LV function) parameters) that might relate to these WSS distribution differences. Aortic diameters, arch angle, LV function parameters (stroke volume, LV ejection fraction, cardiac output) and peak systolic aortic WSS were obtained.

Results

TGA patients had significantly larger neo-aortic root and smaller mid-ascending aorta (AAo) dimensions and aortic arch angle. At rest, patients had significantly higher WSS in the entire thoracic aorta, except for the dilated root. High WSS levels beyond the proximal AAo were associated with the diameter decrease from the root to the mid-AAo (correlation coefficient r = 0.54-0.59, P = 0.022-0.031), not associated with the aortic arch angle. During DS, WSS increased in all aortic segments (P < 0.001), most pronounced in the AAo segments. The increase in LV ejection fraction, stroke volume and cardiac output as a result of DS showed a moderate linear relationship with the WSS increase in the distal AAo (correlation coefficient r = 0.54-0.57, P = 0.002-0.038).

Conclusions

Increased aortic WSS was observed in TGA patients after ASO, related to the ASO-specific geometry, which increased with DS. Stress-enhanced elevated WSS may play a role in neo-aortic root dilatation and anterior aortic wall thinning of the distal AAo.

Introduction

The arterial switch operation (ASO) is the current treatment for patients with transposition of the great arteries (TGA). This surgical intervention restores the ventriculoarterial concordance by reconnecting the great arteries to the correct ventricles leaving the semilunar valves and the native root in its original position. The relocation of the great arteries following ASO results in an altered spatial great artery relationship and geometry of the thoracic aorta. With the Lecompte maneuver, the pulmonary artery bifurcation is positioned in front of the ascending aorta with the pulmonary artery branches embracing the ascending aorta resulting in a more posterior location of the ascending aorta post-ASO. Consequently, an acute angulation of the curvature of the aortic arch is often present after ASO.[1, 2]

In the long term, progressive neo-aortic root dilatation occurs accompanied by an increasing incidence of neo-aortic valve leakage in these patients.[3, 4] Furthermore, cardiothoracic surgeons have observed thinning of the anterior wall of the ascending aorta in adult post-ASO patients who underwent reoperation for the aneurysmatic neo-aortic root dilatation,[5, 6] closely related to the location of the pulmonary arteries. It is largely unknown what mechanisms contribute to the progression of neo-aortic root dilatation and anterior wall thinning, but geometry-driven alterations in aortic flow might have its impact on the (neo-)aortic wall. This relationship has been shown in bicuspid aortic valve-related aortopathy[7] but has not been extensively evaluated in TGA patients post-ASO so far.[8]

With 4D flow magnetic resonance imaging (MRI), blood flow and hemodynamic parameters in large vessels can be visualized and quantified and this imaging modality facilitates studying the relation and interaction of aorta geometry and blood flow on the aortic wall (i.e. wall shear stress, WSS). Currently, almost all patient studies using 4D flow MRI have been performed in rest states. However, it is unknown how aortic blood flow hemodynamics behave with an increase in cardiac output (CO) and whether changes in stroke volume (SV) may add to changes in hemodynamic parameters. Low-dose dobutamine increases heart rate, myocardial contractility and ventricular ejection by stimulating β-1 receptors on the heart and allows studying aortic hemodynamics under increased SV conditions using MRI.

We hypothesize that evaluation of hemodynamics of the thoracic aortic reveals specific areas with abnormal WSS that increase under pharmacological-induced stress conditions and may help to better understand blood flow interactions on the aortic vessel wall in patients with repaired congenital heart diseases with altered aortic geometry. Therefore, the aim of this study was to evaluate aortic WSS in the thoracic aorta of patients with TGA after ASO with comparative rest and pharmacological stress 4D flow MRI investigations.

Methods

Study population

The study protocol was approved by the local Medical Ethics Committee and informed consent was obtained from all patients and their legal guardians. Sixteen patients with TGA and intact ventricular septum or TGA with ventricular septal defect were prospectively included in the study between January 2016 and December 2017. Patients from outpatient pediatric and congenital cardiology clinics who needed a standard-of-care MRI of the heart and large vessels as regular clinical follow-up for early detection of well-known sequelae after ASO from the age of 10 years were invited to participate. To ensure morphologic homogeneity, exclusion criteria were Taussig-Bing anomaly, prior left ventricular (LV) outflow tract obstruction, bicuspid neo-aortic valve, aortic arch obstruction, presence of branch pulmonary artery stent(s), moderate-to-severe neo-aortic insufficiency or prior neo-aortic valve or root reoperations. All patients underwent aortic 4D flow MRI at rest and during dobutamine-induced stress immediately following the standard-of-care MRI assessment. The healthy subjects were recruited from a prior 4D flow MRI validation study[9] and served as a reference group. They underwent the same MRI protocol including 4D flow aortic imaging (only at rest).

Magnetic resonance imaging acquisition

All MRI examinations were performed on a 3T scanner (Ingenia, Philips Healthcare, the Netherlands). The protocol included ECG-gated two-dimensional cine steady-state free precession (SSFP) imaging for ventricular and functional analysis at rest and during dobutamine stress. At rest, a three-dimensional (3D) non-contrast-enhanced magnetic resonance angiography (NCE-MRA) was performed for the assessment of thoracic aorta diameters and aortic arch geometry. 4D flow MRI covering the thoracic aorta was acquired at rest and during dobutamine stress condition. MRI acquisitions details are summarized in supplementary Table S1. Dobutamine was administered intravenously starting at a dose of 5.0 µg/kg/min, and the dose was increased to 7.5 µg/kg/min after 3 min followed by a 5-10 min observation period waiting for a steady state of patients' heart rate and blood pressure.

Aortic geometry and cardiac function

Left ventricular indices [end-systolic and end-diastolic volume (LVESV and LVEDV)] and LV function parameters [SV, LV ejection fraction (LVEF), CO and cardiac index] were obtained from short-axis SSFP-images:

$$Stroke\ volume = \text{LVEDV} - \text{LVESV}; \qquad LVEF = 100 * \frac{stroke\ volume}{LVEDV};$$

$$CO = \text{SV} * \text{heart rate}; \qquad Cardiac\ Index = \frac{\text{CO}}{\text{Body Surface Area}}$$

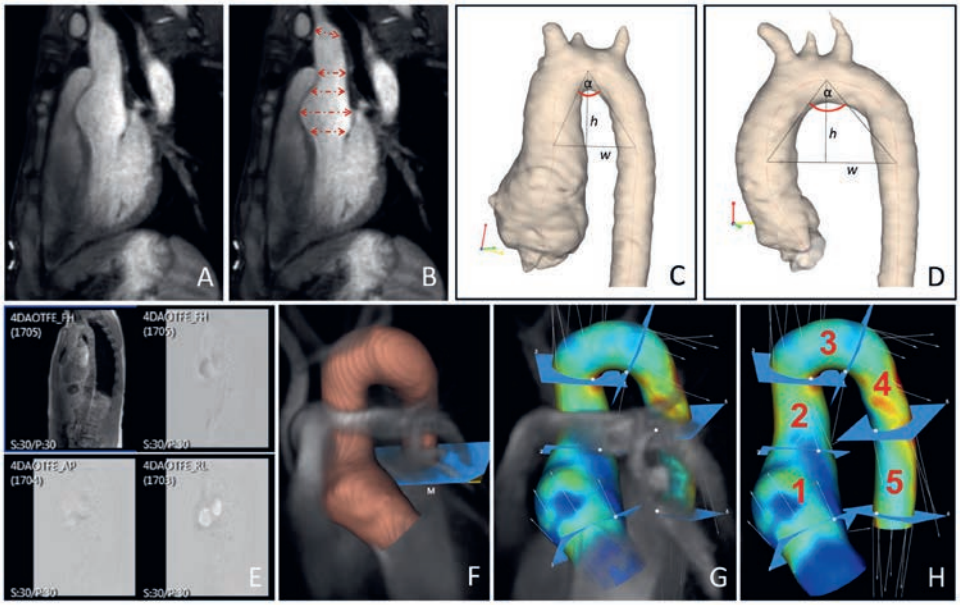

Figure 1. Workflow aortic geometry and 4D flow analysis.
Non-contrast enhanced magnetic resonance angiography (NCE-MRA) (A) with aortic diameter measurements (B). Aortic segmentation from NCE-MRA of a TGA patient (C) and healthy subject (D) with centerline creation, aortic width (*w*), height (*h*) and aortic arch angle (α) measurement. Raw 4D flow MRI data (E) used to create a 3D aortic segmentation (F). Visualization of anatomical great artery relation with the peak systolic aortic WSS (G). Thoracic aorta subdivision into 5 segments (H).

Aortic diameters were measured from NCE-MRA at 6 anatomic landmarks: 1. neo-aortic root (Root); 2. sinotubular junction, defined as the aortic level 5-7 mm below the pulmonary artery bifurcation; 3. mid-ascending aorta at the level of the pulmonary artery bifurcation (mid-AAo); 4. aorta at the origin of the innominate artery; 5. aortic isthmus; 6. mid-descending aorta (Figure 1A-B). Aortic dimensions were measured from external-to-external edges from a sagittal-axis orientation. Average neo-aortic root diameters (average of three cusp-to-commissure dimensions) were measured perpendicular to the aortic axis on NCE-MRA double oblique transversal angulated multiplanar reconstructions. Diameters were indexed to body surface area and converted into Z-scores.[10] Aortic diameter ratio between the neo-aortic root diameter and the mid-AAo diameter was calculated: $\left(\frac{\text{Root}}{\text{mid-AAo}}\right)$.

Aortic arch geometry was obtained from NCE-MRA. After aortic segmentation using Enterprise Suite v6.5 (Vital Images, Minnetonka, USA) and automatic computation of the centerline of the aorta segmentations, the aortic arch width (*w*), maximal height (*h*, perpendicular to the width) and aortic arch angle (α, between mid-AAo, maximal height and mid-descending aorta) were quantified (Figure 1C-D) using an in-house developed software (Python Software Foundation, Wolfeboro Falls, NH, USA). Width-height (*w*/*h*) ratio was calculated accordingly.

Segmental WSS assessment

The software program CAAS MR 4D flow v2.0 (Pie Medical Imaging BV, Maastricht, the Netherlands) was used for post-processing of the 4D flow MRI data, for which a 3D WSS reproducibility analysis study showed robustness of the segmentation and WSS analysis method.[9] A summary of the workflow analysis is depicted in Figure 1E-H, and was previously described in detail.[9] Briefly, from the 4D flow dataset peak systolic thoracic aortic segmentations were performed and provided with an aortic centerline (Figure 1E-F). For the regional aortic wall shear stress (WSS) assessment, the thoracic aorta was manually subdivided into 5 segments based on anatomic landmarks by placing planes perpendicular to the aortic centerline (Figure 1G): segment 1: proximal ascending aorta (pAAo, from aortic valve level to mid-AAo); segment 2: distal ascending aorta (dAAo, from mid-AAo to innominate artery); segment 3: aortic arch (Arch, from the innominate artery until left subclavian artery); segment 4: proximal descending aorta (pDAo, beyond the left subclavian artery to the mid-descending thoracic aorta); and segment 5: distal descending aorta (dDAo, from mid-descending thoracic aorta to the descending aorta at the level of the aortic valve). For every aortic segment, mean 3D systolic WSS (WSSmean) and maximum 3D systolic WSS (WSSmax) values were calculated as described previously (Figure 1H).[9] Wall shear stress is defined as the derivative of the axial velocity u at the vascular wall in the direction perpendicular to the vascular wall times the dynamic viscosity μ (WSS = $\mu \frac{\partial u}{\partial y} \Big|_{y=0}$ (in mPa)). The surface of the 3D segmented aorta was divided into wall points, and for all wall points, a 3D systolic WSS vector was calculated based on a quadratic approximation of the axial velocity profile perpendicular to the surface of the 3D segmented aorta.[9] WSSmax was then defined as the maximum WSS vector of all wall points within the defined aortic segment (in mPa). WSSmean was defined as the average of all WSS vectors of all wall points within the defined aortic segment (in mPa). Differences in WSS (ΔWSS) and percentage WSS changes (%WSS) between rest and stress state were calculated for each segment:

$$\Delta WSS = WSS\ stress - WSS\ rest; \qquad \%WSS = \frac{WSS\ stress - WSS\ rest}{WSS\ rest}$$

Statistical analysis

Statistical analyses were performed using IBM SPSS Statistics version 23 (IBM, Chicago, IL, USA). Variables are presented as mean ± standard deviation or median (interquartile range, IQR) depending on the normality of the distribution. The normality of the distribution was tested using the Shapiro-Wilk test. The primary outcome measure was the WSS distribution along the aortic segments and the WSS change with dobutamine stress in TGA patients. Based on the results, we secondary zoomed in on factors (aortic geometry and LV function parameters) that might relate to these WSS distribution differences. A power calculation was performed to determine the power to detect differences in the WSS values between the rest and dobutamine stress measurements (primary outcome measure). Based on the WSS magnitude known in the healthy pediatric and adult population, study sample sizes to

show a 20% difference (difference of clinical interest; estimated mean difference in WSSmean 400 Pa; estimated standard deviation 100 Pa) in these variables with a power of 90% and a α error of 0.01 (to correct for multiple comparison according to the Bonferroni correction) must contain a minimum of 6 TGA patients. The power analysis was performed for the paired t-test (because of the unknown shape of the underlying distribution) (Division of Biomathematics/Biostatistics, Columbia University Medical Center, New York, USA; http://biomath.info/power). Using the rule of thumb because of using a non-parametric test, we added 15% to the sample size required for a parametric test, resulting in a study sample size of at least 7 to 8 patients.

A chi-square test was performed to investigate differences in sex distribution between TGA patients and healthy subjects. Differences between groups were compared using the independent sample t-test or a Mann Whitney test based on the normality of the distribution. Differences in cardiac parameters between rest and dobutamine stress were tested by a paired t-test; in case of non-normality, the Wilcoxon signed-rank test was performed. A Friedman test was performed to test for differences in the percentage increase in WSS from rest to stress state between the 5 aortic segments. A Bonferroni correction was performed to adjust for the multiple comparisons for the WSS analysis along aortic segments between groups, between rest and dobutamine stress in TGA patients and for the percentage WSS increase from rest to stress between the 5 aortic segments. Correlation between aortic geometry measures (root/mid-AAo diameter ratio, arch angle and *w*/*h* ratio) and segmental aortic WSS were calculated using Spearman rank correlation. Correlation between percentage WSSmean increase and percentage increase in LV function parameters (EF, SV, CO) were calculated using Pearson's correlation. A *P* value <0.05 was considered statistically significant.

Results

Aortic geometry

Patient characteristics are shown in Table 1. Indexed neo-aortic root and sinotubular junction dimensions (Z-scores) were significantly larger in TGA patients compared to healthy subjects. Neo-aortic root and sinotubular junction were dilated (Z-score >2.0) in 94% and 81% of the TGA patients respectively. Patients without aortic Z-score >2.0 had also large indexed neo-aortic root and sinotubular junction dimensions with Z-scores ≥1.7, except for one patient. The mid-AAo diameter was significantly smaller in TGA patients. Other thoracic aortic dimensions were within the normal range compared with the MRI-based healthy reference population (Z-score <2.0). Aortic arch geometry descriptors showed that the aortic arch height was comparable between TGA patients and healthy subjects. The aortic arch angle, aortic width and *w*/*h* ratio were significantly smaller in TGA patients.

Table 1. Baseline characteristics and MRI measurements

	TGA patients (*n* = 16)	Healthy subjects (*n* = 10)	*P* value
Patient and surgical characteristics			
Male, *n* (%)	11 (68.8)	5 (50.0)	0.339
Age, years[a]	16.5 [14.4-18.8]	27.3 [24.9-28.4]	<0.001
Weight, kg	63.8 ± 14.0	68.3 ± 12.7	0.419
Height, cm	173.4 ± 12.7	175.6 ± 6.6	0.571
BSA, m^2	1.75 ± 0.25	1.8 ± 0.20	0.452
Transposition type, *n* (%)			
TGA-IVS	12 (75.0)		
TGA-VSD	4 (25.0)		
Coronary artery anatomy, *n* (%)*			
1LCx-2R	11 (68.8)		
1L-2CxR	2 (12.5)		
1L-2R, *no Cx*	2 (12.5)		
1RL-2Cx	1 (6.3)		
Surgical variables			
Age at ASO, days (range)	8 (1-70)		
Previous surgery prior to ASO, *n* (%)	1 (6.3)		
Lecompte maneuver, *n* (%)	16 (100)		
Coronary artery transfer technique, *n* (%)			
Double button	6 (37.5)		
Single button, single trapdoor	7 (43.8)		
Double trapdoor	3 (18.8)		
Aortic diameters (mm/$BSA^{0.5}$)			
Neo-aortic root sagittal	21.4 ± 3.2	17.0 ± 1.5	0.001
Neo-aortic root short-axis, mean	21.7 ± 3.0	16.7 ± 0.9	<0.001
Sinotubular junction	16.9 ± 3.0	14.1 ± 1.6	0.013
Mid ascending aorta[a]	12.7 [12.0-14.9]	15.1 [13.6-16.3]	0.035
Origin of brachiocephalic trunk	13.0 ± 1.6	13.2 ± 1.2	0.755
Aortic isthmus	12.6 ± 1.6	11.1 ± 1.1	0.018
Mid descending aorta	10.0 ± 1.3	10.2 ± 0.6	0.526
Aortic Z-scores			
Neo-aortic root short-axis, mean	4.8 ± 1.6	1.5 ± 0.7	<0.001
Sinotubular junction	3.6 ± 2.3	1.4 ± 1.3	0.011
Mid-ascending aorta[a]	-0.3 [-1.0-0.3]	1.8 [0.2-2.7]	0.005
Origin of brachiocephalic trunk	-0.5 ± 1.5	0.2 ± 1.3	0.217
Aortic isthmus	2.2 ± 1.2	0.8 ± 1.4	0.013
Mid-descending aorta	-0.3 ± 0.9	0.2 ± 0.6	0.197
Aortic arch geometry			
Arch width	41.3 ± 5.1	58.4 ± 7.4	<0.001
Arch height	31.0 ± 5.5	34.0 ± 3.3	0.132
Arch angle (°)	66.6 ± 8.2	80.1 ± 7.4	<0.001
Width/Height ratio	1.4 ± 0.2	1.7 ± 0.2	0.001

[a] Data are presented as median [Interquartile range]. * Coronary artery anatomy description according to the Leiden Convention coronary coding system. BSA, body surface area; IVS, intact ventricular septum; TGA, transposition of the great arteries; VSD, ventricular septal defect.

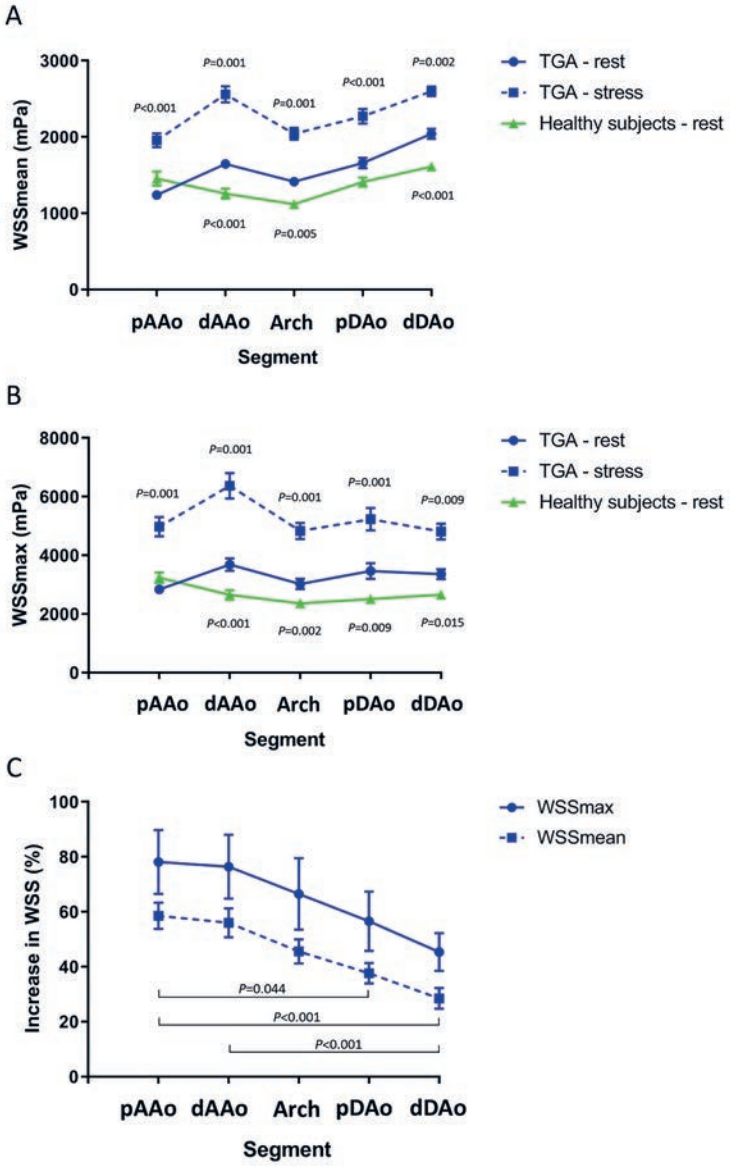

Figure 2. Aortic wall shear stress assessment at rest and during dobutamine stress.
WSSmean (A) and WSSmax (B) values (mean ± standard error of the mean) along the thoracic aortic segments in TGA patients (rest and stress) and compared with healthy subjects (rest). Adjusted *P* values (Bonferroni correction) of the corresponding lines represent the results of the WSS comparison with the TGA patients at rest (only significant *P* values are depicted). Percentage WSS increase between rest and dobutamine stress for each of the thoracic aortic segments (C). Differences in %WSS increase between the 5 segments for WSSmax: $P = 0.19$; for WSSmean: $P < 0.001$ (Friedman test). Brackets with adjusted *P* values (Dunn's pairwise post hoc test with Bonferroni correction) are depicted to indicate statistical significance for differences in %WSSmean increase between the aortic segments.
dAAo, distal ascending aorta; dDAo, distal descending aorta; pAAo, proximal ascending aorta; pDAo, proximal descending aorta; TGA, transposition of the great arteries; WSS, wall shear stress.

Thoracic aortic WSS at rest and correlation with geometry

Figure 2A-B illustrates the aortic WSS along the entire thoracic aortic segments and shows the regional differences in WSSmean and WSSmax between TGA patients and healthy subjects. At rest, TGA patients showed significantly higher WSS in almost all thoracic aortic segments ($P < 0.001$ - $P = 0.015$), except for the pAAo segment (for WSSmean and WSSmax) and pDAo (for WSSmean) (Figure 2A-B). In TGA patients, WSS magnitude (WSSmean and WSSmax) was lowest in the dilated pAAo while the highest WSSmax levels were found in the dAAo segment. Along the thoracic aorta, the trend (i.e. increase or decrease) of the WSSmean and WSSmax between the aortic segments also differed between TGA patients and healthy subjects. In the healthy subjects, there was a WSS decrease from the pAAo segment to the aortic arch segment, with a WSS increase beyond the aortic arch (Figure 2A-B). In TGA patients, there was a significant WSS increase from the pAAo to the dAAo segment ($P < 0.001$ for WSSmean; $P = 0.003$ for WSSmax) with a concomitant WSS decrease in the aortic arch segment compared with the dAAo segment (Figure 2A-B). Beyond the aortic arch, in the descending thoracic aorta, there was overall an increase in WSSmean and WSSmax between the consecutive segments comparable to the trend found in healthy subjects, but on a higher WSS level.

At rest, WSSmean in the dAAo segment, but also in the descending aortic segments, showed a moderate linear relationship with the change in aortic dimension between the neo-aortic root and mid-AAo, as expressed as the root/mid-AAo ratio (Figure 3). A higher systolic WSSmean was detected in the patients with relatively small mid-AAo diameters compared with the neo-aortic root dimensions. In general, the aortic arch geometry descriptors, arch angle and *w*/*h* ratio, did not show a relationship with the WSS parameters from the aortic arch and descending aortic segments (supplementary Table S2). Only for WSSmax in the distal DAo segment, an association was observed with the arch geometry (angle: correlation coefficient r = 0.58, $P = 0.020$ and *w*/*h* ratio: correlation coefficient r = 0.54, $P = 0.032$).

Dobutamine-stress induced changes in LV function parameters

At rest, no significant differences between TGA patients and healthy subjects were observed in cardiac parameters, except for heart rate and cardiac index (supplementary Table S3). All patients received maximum dobutamine dosage (7.5 μg/kg/min) without any adverse effects. In the entire TGA group, heart rate, blood pressure and the LV functional parameters derived from MRI, SV and CO, significantly increased from rest to stress state (supplementary Table S3). Fourteen TGA patients had a normal systolic LV function (EF ≥55%) and two patients slightly below normal (EF 51% and 54%) without regional wall motion abnormalities. No significant neo-aortic regurgitation was present in the patients. All healthy subjects had an EF ≥55%.

Stress-induced changes in aortic WSS and correlation with LV function parameters

During dobutamine stress, the trend in WSS between the aortic segments remained similar but with significantly higher WSS in all aortic segments compared with the levels at rest

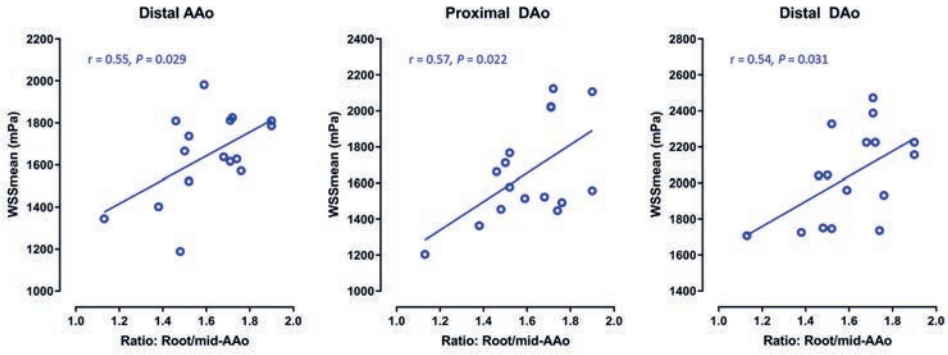

Figure 3. Relationship between ascending aortic diameter change and WSSmean at rest along the thoracic aorta. Spearman correlation coefficient (r).
AAo, ascending aorta; DAo, descending aorta; WSS, wall shear stress.

state ($P < 0.001$ - $P = 0.009$, for WSSmax and WSSmean) (Figure 2A-B). The highest absolute WSSmean and WSSmax values were detected in the dAAo segment. The percentage WSS increase from rest to stress state was highest for the ascending aortic segments (pAAo and dAAo) with a WSS increase between 56-78% (Figure 2C). The percentage WSS increase was the most pronounced for WSSmax and high but to a lesser extend present for WSSmean (for pAAo and dAAo: WSSmax 78% and 76%; WSSmean 58% and 56%, respectively). The dobutamine-induced percentage WSS increase diminished for the consecutive aortic segments beyond the ascending aortic segments (Figure 2C).

All TGA patients showed more or less similar WSS patterns with an increased WSS area at the anterior wall of the dAAo segment, on top of the anterior root. This area of high WSS was present at rest and during dobutamine stress and the area of high WSS also extended over the anterior wall of the dAAo (Figure 4, example of single patient). The WSS distribution in the dAAo segments was asymmetric and more expressed on the anterior wall, and more symmetrically distributed over the aortic wall of descending aortic segments as suggested by the lower magnitude of WSSmax and the higher magnitude of WSSmean in the descending aortic segments as compared with the ascending aortic segments (Figure 2A-B).

The percentage increase of peak systolic WSSmean in the dAAo segment with stress showed a moderate positive linear relationship with the percentage increase in parameters EF, SV and CO as a result of dobutamine (Figure 5). Cardiac output and EF showed the best association with the percentage increase in WSSmean (correlation coefficient r = 0.59, $P = 0.016$ and correlation coefficient r = 0.70, $P = 0.002$, respectively). Arch geometric descriptors did not show significant associations with WSS in aortic segments during dobutamine stress (supplementary Table S2).

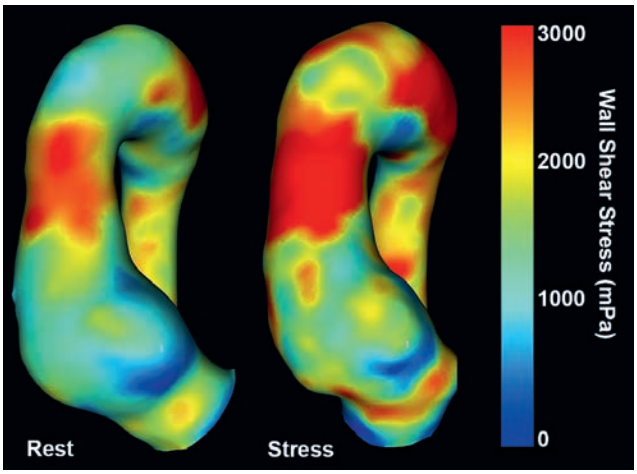

Figure 4. Peak systolic 3D wall shear stress visualization (anterior aortic view) in single a TGA case - rest vs stress

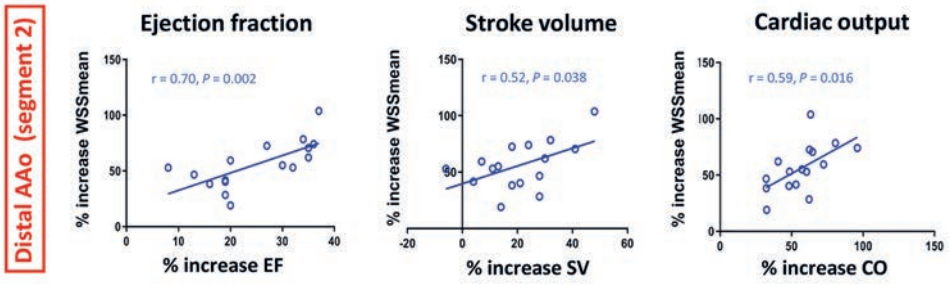

Figure 5. Correlation between increase in WSSmean in the distal AAo and ejection fraction, stroke volume, and cardiac output under dobutamine infusion.
Pearson correlation coefficient (r).
AAo, ascending aorta; CO, cardiac output; EF, ejection fraction; SV, stroke volume; WSS, wall shear stress.

Discussion

This study evaluated the thoracic aortic WSS in TGA patients after ASO. The effect of pharmacological-derived stress on aortic WSS was studied *in vivo* and was compared with the rest state. The main findings of this study demonstrate that patients after ASO have a significantly higher WSS magnitude in the entire thoracic aorta compared with healthy subjects at rest, except for the dilated proximal AAo. The regions of high peak systolic WSS were most pronounced in the distal AAo and located at the anterior aortic wall of that segment. The specific ascending aortic geometry post-ASO, reflected by the size discrepancy

between the dilated neo-aortic root and the smaller mid-AAo diameter, was associated with higher WSS levels in the aortic segments downstream this caliber change: the larger the size discrepancy, the higher the WSS levels in the distal AAo, but also in the descending aortic segments. In addition to this association, the geometry of the aortic arch did not further contribute to the high WSS levels in the aortic arch and the descending aortic segments. Dobutamine-induced cardiac stress did increase WSS magnitude significantly along all thoracic aortic segments, the most prominent in the AAo. The highest peak systolic WSS was present in the distal AAo segment during both rest and stress, but for stress, this was even more pronounced. The peak systolic WSS increase by dobutamine in that segment showed a positive correlation with the increase in the LVEF, SV and CO.

The results of this study extend the findings reported previously.[8] In addition to the increased WSS in the distal AAo segment, significantly higher WSS values at rest were observed in the aortic segments beyond the distal AAo (the arch and descending aortic segments), segments of the aorta remote from the dilated neo-aortic root and not directly affected by the surgical repair. The increased WSS in these descending aortic segments is most likely a perpetuation of the elevated WSS found in the distal AAo segment owing to the eccentric aortic outflow[8] and the abnormal ascending aortic geometry. This is supported by the observed relationship between the ascending aortic geometry and WSS in the descending thoracic aortic segments in this study. Local geometric changes of the aorta (i.e. changes in diameter, arch curvature, vessel torsion) are known to have effect on downstream hemodynamics.[11] In accordance with existing literature,[1,2] TGA patients in this study showed a more acute aortic arch angulation. However, the aortic arch geometry descriptors (angle and *w*/*h* ratio) were not associated with the high WSS magnitude in the aortic arch and descending aortic segments, on top of the aforementioned association with the ascending aortic geometry. This could also be related to the lack of power due to the relatively small sample size of TGA patients.

Impaired aortic bioelastic aortic wall properties have been described after ASO for TGA[12] and may also affect the blood flow propagation in the thoracic aorta (i.e. higher velocity), but these factors were not investigated in this study. In thoracic aortas of healthy volunteers, it has been reported that there is a significant slowing of blood flow velocity in the aortic arch compared with the velocity in the ascending aorta followed by an increase to higher velocities in the descending aorta due to vessel diameter reduction.[13] As WSS is a derivative of velocity, these observations are in accordance to the findings of the WSS trend along the thoracic aorta in the healthy subjects from this study, where WSS initially starts high in the proximal AAo, significantly diminishes in the aortic arch segment and subsequently increases in the descending aortic segments. This trend of WSS increase from the arch to the descending aortic segments was also observed in the TGA patients.

Aortic WSS during dobutamine stress

Low-dose dobutamine administration resulted in a normal cardiac hemodynamic response in the TGA patients. Similar to previous findings from echocardiographic and MRI studies

in healthy subjects,[14, 15] a significant increase in SV and LVEF, a decrease in end-systolic volume and no changes in end-diastolic volume were observed.

The dobutamine-induced increase in SV, EF, and CO enhanced the geometry-driven effects on WSS distribution. The SV in patients after ASO accumulates in the dilated aortic root and under stress may play a role in root dilatation negatively influenced by the smaller mid-AAo segment (vessel narrowing) on top of the dilated root. Notably, highest percentages of WSS increase under stress were found in the proximal and distal AAo segments. The increased WSS findings might introduce a risk with important clinical consequences in the long run as increased WSS is associated with elastic fiber alteration (thinning and degeneration) and dysregulation of the extracellular matrix in the aortic wall.[7, 16] In healthy subjects, regular exercise-induced increases in blood flow and shear stress have been observed to enhance vascular function and structure.[17] However, in diseased aortas with altered flow phenomena and elevated regional WSS aggravated by increased SV, this may have negative effects on cardiovascular remodeling. In the arterial roots of unoperated TGA patients, already structural vessel wall abnormalities characterized by a diminished amount and altered distribution of collagen and a dedifferentiating of smooth muscle cells with increasing age have been observed,[18] making the neo-aortic root theoretically more vulnerable for altered WSS. So far, no reports have been described on histopathological changes in the distal AAo in TGA patients after ASO. However, cardiothoracic surgeons who performed reoperations on adult post-ASO patients have observed a thinner and more fragile anterior wall of the ascending aorta just behind the pulmonary artery bifurcation.[5, 6] These anterior aortic regions clinically correlate with the regions of abnormal increased WSS in the distal AAo as found in this study.

Clinical implications of the altered WSS distribution over the aorta and the changes during stress are preliminary and consequences unknown, as we did not evaluate the effect of it on the aortic wall tissue itself. Correlation studies between 4D flow MR-derived aortic WSS and aortic vessel specimen after neo-aortic root and/or ascending aortic replacement are important next steps to consider. Furthermore, serial 4D flow MR evaluations are essential to assess the predictive value of hemodynamic parameters such as WSS on the progression of aortic dilatation, wall thinning or the development of adverse aortic events (aortic dissection or rupture). Ultimately, comparative hemodynamic studies between TGA patients after ASO performed with different techniques (i.e. conventional ASO with versus without Lecompte maneuver and conventional ASO versus spiral ASO technique) may provide insights for the optimization of surgical strategies for patients with different anatomy. Currently, based on our study, clinical recommendations related to these issues are not yet possible.

Limitations

The study is limited by the small sample size but represents randomly selected TGA patients from the outpatient clinic that required MR investigation as part of their regular lifelong follow-up. Furthermore, healthy subjects in this study were older compared with the TGA

patients. As the velocity of aortic blood flow is known to decrease with increasing age,[19] older age could have lowered the WSS results in healthy subjects since it is a derivative of velocity. However, no large differences in mean velocity and thus in WSS are to be expected based on the small differences in age range between the groups based on a study on the velocity distribution in the normal aorta over age.[19] The comparison of the effect of pharmacological-induced stress on the aortic WSS could not be performed other than within the TGA group.

Conclusion

In conclusion, increased aortic WSS was found in the distal ascending aortic segment and in the aortic segments beyond and was primary related to the ASO-specific geometry of the ascending aorta, not related to the steeper arch geometry. Dobutamine-induced stress further increased abnormal segmental WSS and showed a moderate positive correlation with the increase in left ventricular cardiac output parameters. Pharmacological-induced stress evaluations of aortic blood flow may better reflect location and expansion of vascular wall areas exposed to abnormal WSS with subsequent risks for vascular remodeling. Stress might play a role in neo-aortic root dilatation in TGA patients after ASO given the significant stress-induced WSS increase in the neo-aortic root, acting on root tissue with structural vessel wall abnormalities.

ACKNOWLEDGEMENT

The authors thank Pieter J. van den Boogaard for help in providing support with the MRI acquisitions, dr. Monique R.M. Jongbloed for the assistance with adult patient enrollment and Alex Korenhof for the support in post-processing of the MRI data.

References

1. Ntsinjana HN, Capelli C, Biglino G, Cook AC, Tann O, Derrick G, Taylor AM, Schievano S. 3D morphometric analysis of the arterial switch operation using in vivo MRI data. *Clin Anat*. 2014;27(8):1212-22.
2. Martins D, Khraiche D, Legendre A, Boddaert N, Raisky O, Bonnet D, Raimondi F. Aortic angle is associated with neo-aortic root dilatation and regurgitation following arterial switch operation. *Int J Cardiol*. 2019;280:53-6.
3. Lo Rito M, Fittipaldi M, Haththotuwa R, Jones TJ, Khan N, Clift P, Brawn WJ, Barron DJ. Long-term fate of the aortic valve after an arterial switch operation. *J Thorac Cardiovasc Surg*. 2015;149(4):1089-94.
4. van der Palen RLF, van der Bom T, Dekker A, Tsonaka R, van Geloven N, Kuipers IM, Konings TC, Rammeloo LAJ, Ten Harkel ADJ, Jongbloed MRM, et al. Progression of aortic root dilatation and aortic valve regurgitation after the arterial switch operation. *Heart*. 2019;105(22):1732-40.
5. Koolbergen DR, Manshanden JS, Yazdanbakhsh AP, Bouma BJ, Blom NA, de Mol BA, Mulder BJ, Hazekamp MG. Reoperation for neoaortic root pathology after the arterial switch operation. *Eur J Cardiothorac Surg*. 2014;46(3):474-9.
6. Vida VL, Zanotto L, Zanotto L, Stellin G, European Congenital Heart Surgeons Association Study G, Padalino M, Sarris G, Protopapas E, Prospero C, Pizarro C, et al. Left-Sided Reoperations After Arterial Switch Operation: A European Multicenter Study. *Ann Thorac Surg*. 2017;104(3):899-906.
7. Guzzardi DG, Barker AJ, van Ooij P, Malaisrie SC, Puthumana JJ, Belke DD, Mewhort HE, Svystonyuk DA, Kang S, Verma S, et al. Valve-Related Hemodynamics Mediate Human Bicuspid Aortopathy: Insights From Wall Shear Stress Mapping. *J Am Coll Cardiol*. 2015;66(8):892-900.
8. van der Palen RLF, Deurvorst QS, Kroft LJM, van den Boogaard PJ, Hazekamp MG, Blom NA, Lamb HJ, Westenberg JJM, Roest AAW. Altered Ascending Aorta Hemodynamics in Patients After Arterial Switch Operation for Transposition of the Great Arteries. *J Magn Reson Imaging*. 2020;51(4):1105-16.
9. van der Palen RLF, Roest AAW, van den Boogaard PJ, de Roos A, Blom NA, Westenberg JJM. Scan-rescan reproducibility of segmental aortic wall shear stress as assessed by phase-specific segmentation with 4D flow MRI in healthy volunteers. *MAGMA*. 2018;31(5):653-63.
10. Kaiser T, Kellenberger CJ, Albisetti M, Bergstrasser E, Valsangiacomo Buechel ER. Normal values for aortic diameters in children and adolescents--assessment in vivo by contrast-enhanced CMR-angiography. *J Cardiovasc Magn Reson*. 2008;10:56.
11. Prahl Wittberg L, van Wyk S, Fuchs L, Gutmark E, Backeljauw P, Gutmark-Little I. Effects of aortic irregularities on blood flow. *Biomech Model Mechanobiol*. 2016;15(2):345-60.
12. Voges I, Jerosch-Herold M, Hedderich J, Hart C, Petko C, Scheewe J, Andrade AC, Pham M, Gabbert D, Kramer HH, et al. Implications of early aortic stiffening in patients with transposition of the great arteries after arterial switch operation. *Circ Cardiovasc Imaging*. 2013;6(2):245-53.
13. Hope TA, Markl M, Wigstrom L, Alley MT, Miller DC, Herfkens RJ. Comparison of flow patterns in ascending aortic aneurysms and volunteers using four-dimensional magnetic resonance velocity mapping. *J Magn Reson Imaging*. 2007;26(6):1471-9.
14. De Wolf D, Suys B, Verhaaren H, Matthys D, Taeymans Y. Low-dose dobutamine stress echocardiography in children and young adults. *Am J Cardiol*. 1998;81(7):895-901.
15. Parish V, Valverde I, Kutty S, Head C, Qureshi SA, Sarikouch S, Greil G, Schaeffter T, Razavi R, Beerbaum P. Dobutamine stress MRI in repaired tetralogy of Fallot with chronic pulmonary regurgitation: a comparison with healthy volunteers. *Int J Cardiol*. 2013;166(1):96-105.
16. Bollache E, Guzzardi DG, Sattari S, Olsen KE, Di Martino ES, Malaisrie SC, van Ooij P, Collins J, Carr J, McCarthy PM, et al. Aortic valve-mediated wall shear stress is heterogeneous and predicts regional aortic elastic fiber thinning in bicuspid aortic valve-associated aortopathy. *J Thorac Cardiovasc Surg*. 2018;156(6):2112-20 e2.

17. Niebauer J, Cooke JP. Cardiovascular effects of exercise: role of endothelial shear stress. *J Am Coll Cardiol*. 1996;28(7):1652-60.

18. Lalezari S, Mahtab EA, Bartelings MM, Wisse LJ, Hazekamp MG, Gittenberger-de Groot AC. The outflow tract in transposition of the great arteries: an anatomic and morphologic study. *Ann Thorac Surg*. 2009;88(4):1300-5.

19. Garcia J, van der Palen RLF, Bollache E, Jarvis K, Rose MJ, Barker AJ, Collins JD, Carr JC, Robinson J, Rigsby CK, et al. Distribution of blood flow velocity in the normal aorta: Effect of age and gender. *J Magn Reson Imaging*. 2018;47(2):487-98.

Supplementary material

Supplementary Table S1. NCE-MRA and 4D flow MRI acquisition details

MR scanner, field strength	Ingenia - Philips Medical Systems, 3Tesla
Coil	Combination of FlexCoverage Posterior coil (table top) and dStream Torso coil, providing up to 32 coil elements for signal reception
NCE-MRA	
Sequence	Dixon
Respiratory compensation	Navigator gating
Cardiac gating	Prospective, to end diastole
Spatial resolution (mm)	1.6 x 1.6 x 3.2
Temporal resolution (ms)	31.4 ± 1.6
TE (ms)	2.3
TR (ms)	3.6-3.9
Field-of-view (mm)	300 x 300 x 99
Reconstructed voxel size (mm)	0.8 x 0.8 x 1.6
Aortic 4D flow MRI	
Sequence	Segmented fast-spoiled echo pulse
Respiratory compensation	Navigator gating
Cardiac gating	retrospective, 24-36 phases
Spatial resolution (mm)	2.5 x 2.5 x 2.5
Temporal resolution (ms)	34-36 (rest)
	33-34 (stress)
Flip angle (°)	10
TE (ms)	2.4-2.6 (rest)
	2.2-2.4 (stress)
TR (ms)	4.2-4.5 (rest)
	4.1-4.3 (stress)
VENC (cm/s)	200 (range 200-300) (rest)
	3000 (range 250-350) (stress)
Scan duration (minutes)	10-12
Acceleration methods	SENSE factor 2.5, AP direction; TFE factor 2
Gradient correction	Yes*
Phase offset correction	Yes*
Acquisition time	~ 12 minutes

* from standard available scanner software.
AP, anterior-posterior; ms, milliseconds; NCE-MRA, non-contrast enhanced magnetic resonance angiography; SENSE, sensitivity encoding; TE, echo time; TFE, turbo field echo; TR, repetition time; VENC, velocity encoding.

Supplementary Table S2. Relationship between the aortic arch geometry and aortic WSS in TGA patients from the arch and beyond

		Arch angle (°)		***w/h* ratio**	
		r	***P* value**	**r**	***P* value**
Rest state					
Arch	WSSmean	0.01	0.97	-0.08	0.76
	WSSmax	0.11	0.69	0.03	0.91
pDAo	WSSmean	0.24	0.36	0.19	0.49
	WSSmax	0.35	0.19	0.25	0.34
dDAo	WSSmean	0.13	0.64	0.13	0.63
	WSSmax*	0.58	0.02	0.54	0.03
Stress state					
Arch	WSSmean	-0.01	0.96	-0.08	0.77
	WSSmax	0.24	0.38	0.27	0.31
pDAo	WSSmean	0.004	0.99	-0.01	0.96
	WSSmax	-0.02	0.95	0.02	0.94
dDAo	WSSmean	-0.35	0.19	-0.25	0.35
	WSSmax	0.28	0.30	0.32	0.23

Spearman correlation coefficient (r). * statistically significant.
dDAo, distal descending aorta; pDAo, proximal descending aorta; WSSmax, maximum 3D systolic wall shear stress; WSSmean, mean 3D systolic wall shear stress.

Supplementary Table S3. Blood pressure, heart rate and MRI measurements during rest and stress

	TGA patients				Healthy subjects	*P* value	
	Rest	Stress	Difference Rest-Stress		Rest	TGA vs Healthy at rest	TGA: rest vs stress state
	Mean (SD)	*Mean (SD)*	*Δ (SD)*	*% (SD)*	*Mean (SD)*		
HR (bpm)	72.3 (12.3)	98.3 (17.8)	27.2 (14.6)	40.0 (22.0)	60.8 (7.7)	0.015	<0.001
SBP (mmHg)	123.4 (14.1)	165.8 (18.7)	41.8 (19.7)	35.1 (15.4)	NA	NA	<0.001
DBP (mmHg)	61.8 (9.7)	69.1 (10.1)	7.3 (10.9)	13.4 (18.7)	NA	NA	0.017
EDV (ml)	171.9 (44.7)	165.7 (45.1)	-6.3 (14.9)	-3.4 (8.8)	161.3 (35.9)	0.531	0.114
EDVi (ml/m^2)	97.9 (18.5)	94.7 (20.6)	-3.1 (8.2)	-3.4 (8.8)	88.0 (12.5)	0.151	0.142
ESV (ml)	69.0 (23.7)	43.4 (15.7)	-25.6 (10.1)	-36.6 (9.3)	60.0 (13.1)	0.283	<0.001
ESVi (ml/m^2)	38.9 (10.0)	24.6 (7.1)	-14.2 (4.5)	-36.6 (9.3)	32.8 (5.0)	0.051	<0.001
SV (ml)	101.7 (24.2)	122.1 (30.2)	20.4 (15.9)	20.6 (13.9)	100.3 (21.5)	0.882	<0.001
SVi (ml/m^2)	58.3 (11.6)	70.0 (14.2)	11.6 (8.1)	20.6 (13.9)	54.7 (6.9)	0.382	<0.001
EF (%)	59.7 (5.5)	74.2 (3.4)	14.5 (4.6)	25.0 (9.2)	62.3 (2.5)	0.181	<0.001
CO (l/min)	7.2 (1.5)	11.2 (2.4)	4.0 (1.3)	56.7 (17.8)	6.1 (1.2)	0.066	<0.001
CI (l/min/m^2)	4.2 (0.8)	6.4 (1.0)	2.3 (0.5)	56.7 (17.8)	3.4 (0.5)	0.011	<0.001

CO, cardiac output; CI, cardiac output indexed for body surface area; DPB, diastolic blood pressure; EDV, end-diastolic volume; EDVi, end-diastolic volume indexed for body surface area; EF, ejection fraction; ESV, end-systolic volume; ESVi, end-systolic volume indexed for body surface area; HR, Heart rate; NA, not available; SBP, systolic blood pressure; SV, stroke volume; SVi, stroke volume indexed for body surface area; TGA, transposition of the great arteries.